



Energy conservation and heat dissipation by maximizing convection heat flow in a channel with particulate media

S.M.Prabhu*¹, Abbas Moinudeen²

¹SK Fomra Institute of Technology, Chennai - 600 121, (INDIA)

²Satyabhama University, Chennai - 600 112, (INDIA)

Received: 1st June, 2010 ; Accepted: 10th June, 2010

ABSTRACT

Here we discuss the experimental results for flow due to gravitational porous multiblock porous media. These are applied in Electronic packages (Linear and hybrid Integrated Circuits). A Brinkman extended Darcy model and a semiheuristic energy model is obtained by relaxing the local thermal equilibrium(LTE)assumption are adopted. Aluminium foam samples of different pore sizes(5-60PPI) and porosities(0.8-0.99) were used to illustrate the effects of metal foam geometry on heat transfer. Energy concentration is done by porous cavities in the prous media for energy savings and enrgy distribution. © 2009 Trade Science Inc. - INDIA

INTRODUCTION

The Flow and transport at interface between a porous medium and clear fluid is very important in digital Integrated circuits and heatpacks with high energy packed into a small volume(eg. IC Engines of two wheelers, hot beverages with heat packed insulated vessel. The mechanisms that contribute to the enhanced heat transfer include heat conduction in the metal foam matrix (whose conductivity is always higher by several orders of magnitude. The well known Darcy's law is based on a balance between the present gradient and the viscous forces and breaks down for high velocities when inertia terms are no longer negligible. Here we present numerical and experimental results for buoyancy induced flow in a high porosity metal foam. Energy concentration is done by porous cavities in the prous media for energy savings and enrgy distribution

Energy is conserved, and distributed to cooler areas of process when desired thus saving energy and heat in large quantities

EXPERIMENTAL METHODS

The metal foam heat sink was tested under several Convection conditions in a horizontal configuration. Figure 1 shows the experimental setup for the foam heating in a transparent enclosure. A large-scale transparent glass setup housing of 0.45m ht and width of 0.31m deep. Holes were drilled on the base of the samples to insert cartridge heaters. The base of cartridge was insulated using styrene foam . The experimental setup has=d the heater arrangement with $L_{i=2} L_r=14$, $W=1.1/H=1$, $Re=500$, $Ri=50$, $Pr=06$.

These values are suitably selected for satisfying the geometry and transfer requirements of electronic IC packages

The area of the block is 6cmx6cm, The cartridge was heated by a 5w heater coil, the values of temperatures were found by thermocouple connected to temperature recorder switch. During a typical experimental run the powers were varied tom achieve different base late temperature and hence Rayleigh numbers. Due to temperature constraints the parameters of the heat

Full Paper

input were restricted to maximum base plate temperature of 80*c

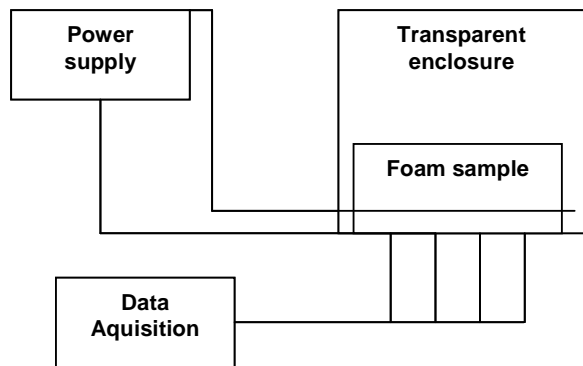


Figure 1 : Metal foam sample experiments experimental setup

The heat transfer coefficient was calculated by the Newton's law of cooling

MATHEMATICAL MODEL

Consider a metal foam sample heated from above. The foam sample is saturated with & surrounded by a fluid, which extends a distance s1 in x direction and s2 in y direction

The steady two dimensional equations for the fluid saturated porous medium & for the clear fluid region outside the metal foam are written separately as shown below

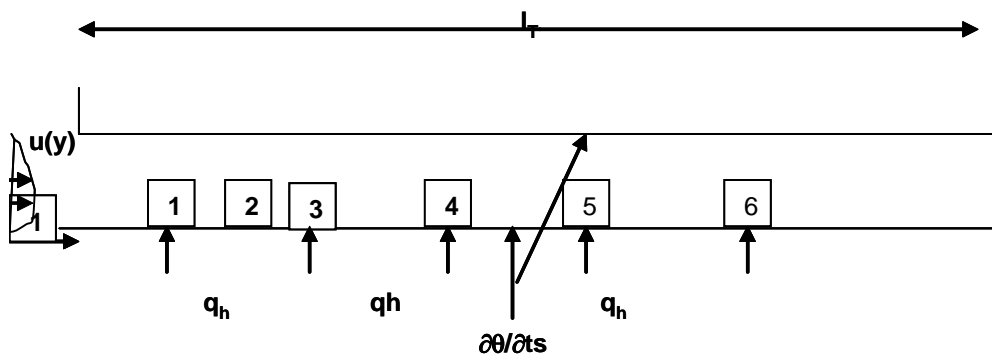


Figure 2 : Schematic of Porous bed (ref Figure 1)

Continuity and momentum equations for porous medium

For a fluid passage with a constant at arbitrary shaped cross section the Brinkman momentum eqn is given by

$$\mu \left(\frac{\partial^2 u}{\partial z^2} + \frac{\partial^2 u}{\partial x^2} \right) - \frac{\mu u}{K} - \frac{\partial p}{\partial x} = 0 \tag{1}$$

leads towards computation of fully developed velocity profile in which the pressure gradient $\phi = \partial p / \partial x$ is a constant. The dimensionless form of eq(1) is

$$M \left(\partial^2 u / \partial y^2 + \partial^2 u / \partial z^2 \right) - u / da - 1 = 0 \tag{2}$$

Where $y = y / L_{c,z=z/L}$, $M = \mu_e / \mu$, $u = \mu u / \phi L_c^2$ and $Da = K / L_c^2$ is the Darcy number. Moreover μ_e is the effective viscosity, K the permeability and L_c is chosen as arbitrary length. The solution of eq(2) with the boundary condition $u=0$ at the wall is often obtainable using variational calculus, & by definition the mean velocity is

$$U = \frac{1}{A} \int u dA \tag{3}$$

Governing energy equation

Under steady state conditions & when

thermophysical properties are independent of temperature, the energy eqn for fully developed flow is

$$\rho C_p \partial T / \partial x = \partial / \partial x (k_s \partial T / \partial x) + k_s \partial / \partial y (\partial T / \partial y) + k_s \partial / \partial z (\partial T / \partial z) + S(x,y,z) \tag{4}$$

where volumetric heat sources (x,y,z) represents the contribution of frictional heating. The parameters ρC_p & k_e may depend on y & z but remain independent of x . More importantly the contribution of axial conduction deferred to the subsequent is neglected, hence eq(4) reduces

$$k_s \partial / \partial y (\partial T / \partial y) + k_s \partial / \partial z (\partial T / \partial z) + S(x,y,z) = \rho C_p \partial T / \partial x \tag{5}$$

The objective is to delineate the heat transfer characteristics when the above two techniques are applied at the same time, i.e enforcing periodic in the flow.

Continuity & momentum equations for the porous medium

$$\nabla \cdot \langle V \rangle = 0$$

$$\frac{1}{\epsilon} \frac{\partial \langle V \rangle}{\partial t} + \frac{\Delta \langle V \rangle \cdot \langle V \rangle}{\epsilon} = -\Delta \langle V \rangle + g + v \cdot \nabla^2 \langle V \rangle - \epsilon \left(\frac{v}{K} + \frac{F |v|}{K^{0.5}} \right) \langle v \rangle \tag{7}$$

Fluid phase energy equation in the porous medium

$$\varepsilon(\rho c_p)_f \frac{\partial T_f}{\partial \tau} + \nabla \cdot [k_{fe} + k_d] \nabla T_f + \langle \rho c_p \rangle_f \langle \mathbf{v} \rangle \cdot \nabla T_f = h_{sf} a_{sf} (T_s - T_f) \quad (8)$$

Solid phase energy equation in the porous medium

$$(1-\varepsilon)(\rho c_p)_s \frac{\partial T_s}{\partial \tau} = \nabla \cdot (k_{sf} \nabla T_s) - h_{sf} a_{sf} (T_s - T_f) \quad (9)$$

Continuity & momentum equation for clear fluid region

$$\nabla \cdot \mathbf{v} = 0 \quad (10)$$

$$\partial \mathbf{v} + \mathbf{v} \cdot \nabla \mathbf{v} = -1 \nabla p + \mathbf{g} + \nu \nabla^2 \mathbf{v} \quad (11)$$

Energy equation for the clear fluid region

$$(\rho c_p)_f \left(\frac{\partial T_f}{\partial \tau} + \mathbf{v} \cdot \nabla T_f \right) = \nabla \cdot (k_f \nabla T_f) \quad (12)$$

where indices s & f denote the solid and fluid phases respectively. $\langle \varphi \rangle$ is the local volume average of a quantity φ , k_{fe} , k_{se} are the thermal conductivities for fluid and solid respectively, and F denotes a geometric factor. In eq(3) the dispersion conductivity k_d is assumed to be isotropic and is expressed as

$$k_d = (\rho c_p)_f C_D \sqrt{K} |\langle \mathbf{v} \rangle| \quad (13)$$

In eqns(3) & (4) the energy equations for the porous medium are coupled by the interfacial term, which represents the heat transfer between the two phases via the fluid to solid heat transfer coefficient, h_{sf} interfacial area a_{sf} .

For $Re \sim 100-1000$,

$$a_{sf} = 3\pi d_f \left\{ 1 - \exp\left(\frac{-(1-\varepsilon)}{0.04}\right) \right\} \quad (14)$$

$$\text{At } x=0, u = \frac{6y}{H} \left(\frac{1-y}{H} \right), v=0, T_f=0 \text{ for } 0 < y < H \quad (15)$$

$$\text{At } x=L, \partial \varphi / \partial x = 0 \quad (\varphi = u, v, T_f, T_s) \text{ for } 0 < y < H \quad (16a)$$

$$\text{At } y=H, u=v=0 \text{ for } 0 < x < L \quad (16b)$$

$$-\left(k_{fe} \frac{\partial T_f}{\partial y} + k_{se} \frac{\partial T_s}{\partial y} \right)_{y=0} = q_h \text{ for heaters 2 \& 5}$$

$$-\left(k_{fe} \frac{\partial T_f}{\partial y} + k_{se} \frac{\partial T_s}{\partial y} \right)_{y=0} = q_h \Delta q_h \sin(2\pi\omega t) \text{ for heater 1}$$

$$\frac{\partial T_f}{\partial y} = \frac{\partial T_s}{\partial y} = 0 \text{ for } 0 < x < L \text{ except the regions of heaters} \quad (16c)$$

where ω is the dimensional frequency & Δq_h denotes dimensional amplitude of thermal modulation at heater 1. An additional boundary is required to solve coupled en-

ergy equations of solid/fluid phase in the porous medium. This is obtained from the local thermal equilibrium assumption at the heated wall i.e. $T_{f/wall} \sim T_{s/wall} = T_w$

It should be mentioned that there are conceptual difficulties associated with specification of heat flux boundary condition while using the two equation model or temperature. In present study, the boundary condition (14b) is based on the assumption that the total heat flux is divided between the solid and fluid phases following the effective conductivities for the two phases.

Also at the interface between porous medium & clear fluid, the conditions are

$$u|_L = u|_{L+}, v|_L = v|_{L+}, p|_L = p|_{L+} \quad (17a)$$

$$[\varepsilon T_f + (1-\varepsilon) T_s]|_L = T_f|_{L+} \quad (17b)$$

$$-\left(k_{fe} \frac{\partial T_f}{\partial y} + k_{se} \frac{\partial T_s}{\partial y} \right)_{y=0} = q_h \Delta q_h \sin(2\pi\omega t) \text{ for heater 1}$$

$$\frac{1}{\varepsilon} \left(\frac{\partial U}{\partial \tau} + \frac{U \partial U}{\partial X} + \frac{V \partial U}{\partial Y} \right) = -\frac{1}{\rho \partial X} \frac{\partial P}{\partial X} + \frac{1}{Re} \nabla^2 U - \varepsilon \varphi \left(\frac{1}{Da Re} + \frac{F |V|}{Da^{1/2}} \right) U \quad (18)$$

$$\frac{1}{\varepsilon} \left(\frac{\partial U}{\partial \tau} + \frac{U \partial U}{\partial X} + \frac{V \partial U}{\partial Y} \right) = -\frac{1}{\rho \partial X} \frac{\partial P}{\partial X} + \frac{Ra \theta}{Re^2 Pr} + \frac{1}{Re} \nabla^2 U - \varepsilon \varphi \left(\frac{1}{Da Re} + \frac{F |V|}{Da^{1/2}} \right) V \quad (19)$$

Energy Equations

$$\frac{1}{\varepsilon} \left(\frac{\partial U}{\partial \tau} + \frac{U \partial U}{\partial X} + \frac{V \partial U}{\partial Y} \right) = -\frac{1}{Re Pr} [(\lambda_{fe} + \lambda_d) \varphi - (\varphi - 1) \nabla^2 \theta + \frac{\varphi \lambda Bi_f}{Re Pr} (\theta_s - \theta_f)] \quad (18)$$

$$\frac{1}{\varepsilon} \left(\frac{\partial U}{\partial \tau} + \frac{U \partial U}{\partial X} + \frac{V \partial U}{\partial Y} \right) = -\frac{\lambda_{se} \nabla^2 \theta}{Re Pr} + \frac{\varphi \lambda Bi_f}{Re Pr} (\theta_s - \theta_f) \quad (19)$$

where $Da = K/H^2$; $Bi_f = \frac{h_{sf} a_{sf} H^2}{k_{se}}$

$$Bi_s = \frac{h_{sf} a_{sf} H^2}{k_{fe}} \quad Ra = \frac{g \beta q_h H^4}{\nu_f \alpha_f}$$

$$\alpha = k/\rho c_p, Re = uH/\nu, \lambda_{fe} = k_{fe}/k_f, \lambda_{se} = k_{se}/k_f; \lambda_d = k_d/k_f$$

The nondimensional B. condns & interface matching conditions can be derived from (16). The nondimensional thermal condition at heater 1 is given by

Full Paper

$$\frac{\lambda \partial \theta}{\partial Y} - \frac{\lambda \partial \theta}{\partial Y} = 1 + \delta \sin(\pi \omega \tau)$$

where $\omega = \omega H / u_1$ the nondimensional frequency; $\delta = \Delta q_h / q_h$ denote nondimensional amplitude of thermal modulation at heater 1

dimensionless friction factor $f = (\Delta p / L_T) (D_h / \rho u^2)$

A performance evaluation criterion, G is introduced which weighs the gain in heat transfer against price to pay in terms of pumping power(16). It is defined as the relative merit of protruded blocks in comparison to smooth channel with flush mounted heaters(denoted by subscript 0)

$$G = \frac{Nu_s / Nu_0}{(f_s / f_0)^{1/3}} \tag{6}$$

The objective is to delineate the heat transfer characteristics when the above two techniques are applies at the same time, i.e enforcing periodicity in the flow. The experimental setup has=d the heater arrangement with $L_{1=2} L_T = 14, W = 1.1/H = 1, Re = 500, Ri = 50, Pr = 06.$

For flow over a rectangular duct heat transfer coefficient is given by(2)

$$h = 0.023 * k * Nre^{0.7} Npr^{0.3} / L = 0.023 * 0.43 * 500^{0.7} * 0.93^{0.3} / 3 = 1.37 \text{ w/sqm} * c$$

h (at $T = 40 * C$) = 1.66

$$Nu = h d_s / k_{f=1.37} = 1.37 * 0.5 / 0.43 = 1.805$$

$$Nu_0 = h_{(at T=40C)} d_s / k_{f=1.37} = 1.37 * 0.5 / 0.43 = 1.805$$

For Basic state (Non modulating flow) we have $\delta = 0$

$$Nu_s = \frac{H}{1} \int \left(\frac{q_h H}{(T_w - T_o) k_f} \right) dX = \frac{H}{1} \frac{1}{\theta} dx$$

For Non modulating flow $\delta \neq 0$

TABLE 1 : Properties of aluminium foam used in above setup (length of the chip =3cm)

PPI	d _f cm	d _p cm	k _{se}	K=π d _p cm ²	Temperature *c	F	Da
5	0.05	0.43	0.02	0.15	85	0.04	0.002
10	0.08	0.9	0.04	0.24	91	0.0422	0.0032
20	0.12	1.13	0.06	0.29	98	0.024	0.0051
40	0.193	1.22	0.1	0.333	105	0.033	0.006

TABLE 2 : Nusselt numbers and dimensionless criterion G_{s(eq)} (No of heaters =5)

Heater dist from entripoint cm	h w/sqm*c	Non modulating case (δ=0)			modulating case (δ=1)			Temperature *c	Heat flux Kw/sqm
		Nu=hd _s /k _f	f _s	G=(Nu _s /Nu ₀)/(f _s /f ₀) ^{1/3}	Nu _{av}	f _{av} =Σ f _s /5	G=(Nu _s /Nu ₀)/(f _s /f ₀) ^{1/3}		
1	1.37	1.805	0.02	1.08	1.32	0.013	1.33	85	2.99
2	1.54	2.21	0.017	1.12	1.43	0.011	1.45	91	2.94
3.5	1.64	2.54	0.033	1.21	1.23	0.007	1.54	98	2.31
6	1.33	2.77	0.016	1.32	1.77	0.003	1.65	105	1.98

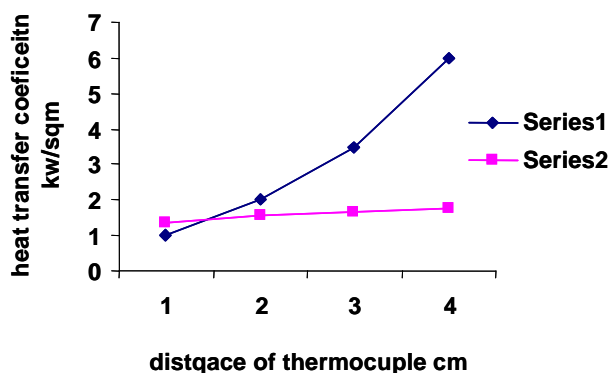


Figure 3 : Plot of dist from heatend vs heat tr coef

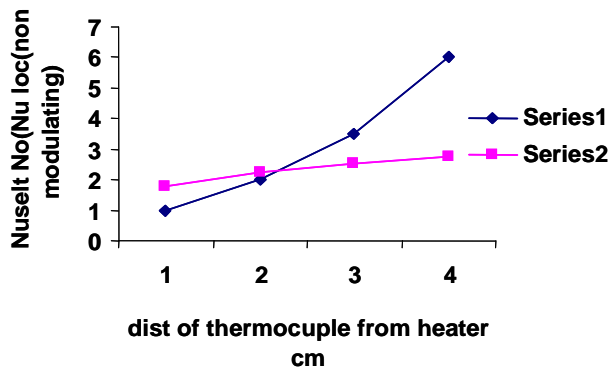


Figure 4 : Plot of nulocal (non modulating case)

RESULTS AND DISCUSSION

The experimental setup has the heater arrangement with $L_{1=2} L_T = 14 W = 1.1/H = 1, Re = 500, Ri = 50, Pr = 06.$ These values are suitably selected for satisfying the

geometry and transfer requirements of electronic IC packages. A concern in practical utilization of protruded porous blocks is the increased flow resistance, which leads to increased pumping requirement. The calculations of various parameters like Nusselt No, Evaluation criterion, friction factor & transfer coefficient for non

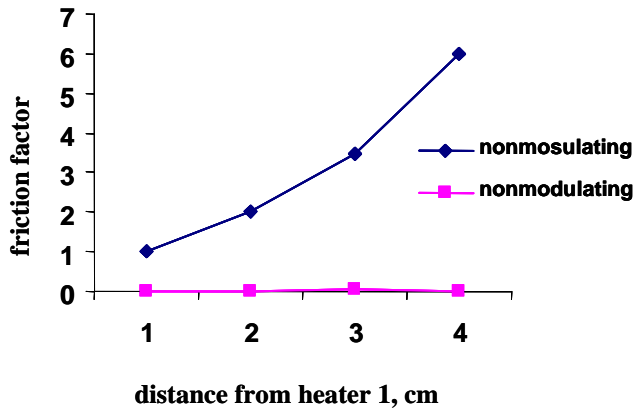


Figure 5 : Plot of friction factor vs dist from heater 1(non modulating case)

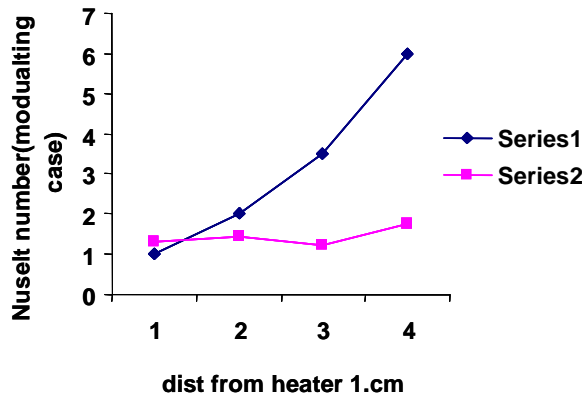


Figure 7 : Nuselt No (modulating case)

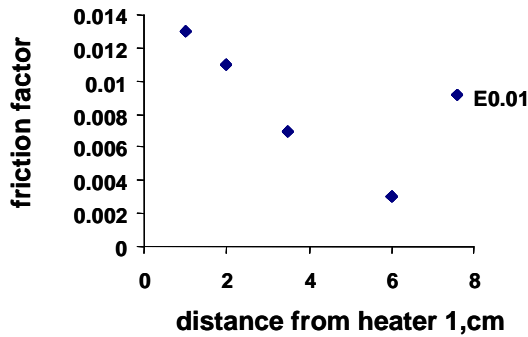


Figure 9 : Dist from heater 1 vs friction factor (modulating case)

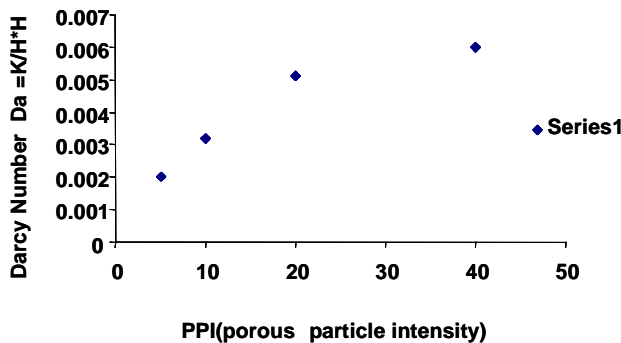


Figure 11 : PPI vs darcy number

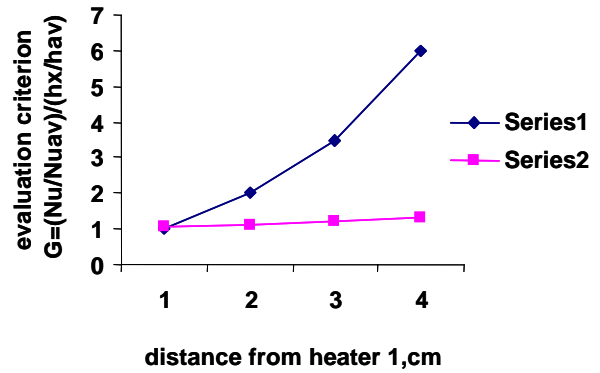


Figure 6 : Evaluation criterion vs distance from heater 1 cm

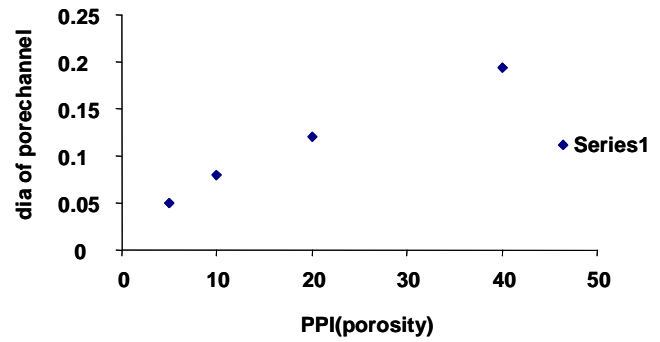


Figure 8 : Plot of PPI(porosity) vs dia of pore channel

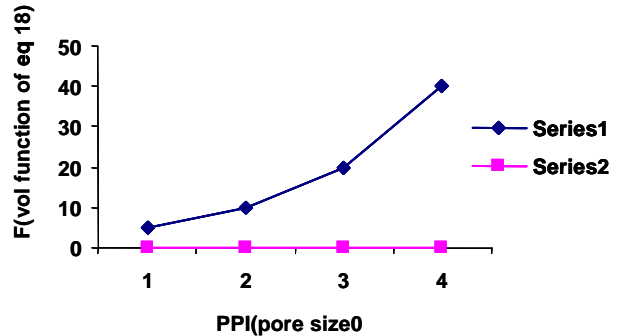


Figure 10 : Plot of PPI vs F (volume function eq 18)

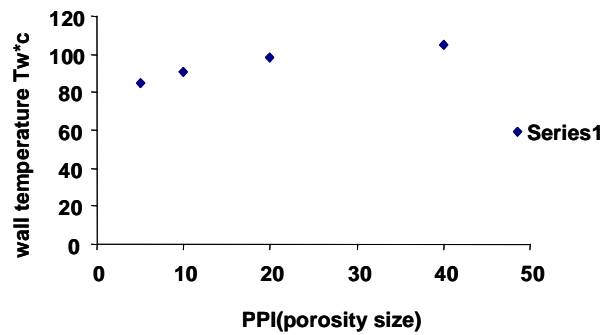


Figure 12 : Plot of PPI vs wall temperature

modulating($\delta \neq 0$)&, modulating($\delta = 0$) were computed for varying distance from heater 1 in TABLE 1. The properties of Aluminium porous foams for different PPI like wall temperature, heat flux, pore channel diameter, area of contact and Darcy Number were collected and are

Full Paper

shown in TABLE 2. Figures 1-4 show plots of distance from heater 1 with of Nusselt No, Evaluation criterion, friction factor & transfer coefficient for non modulating ($\delta \neq 0$) & figures 5-7 for modulating ($\delta = 0$). Figures 8-12 show variation of Darcy number, diameter of channel pore and volume Function $F(v)$ (of eq18) for various PPI (pores per inch) are shown

CONCLUSIONS & SUGGESTIONS

Heat transfer with porous blocks attached than for a smooth channel with flush mounted heaters. Also Nu_s at heater increases appreciably as the pore density increases appreciably as the pore density decreases. This can be explained by noting that the flow resistance decreases as pore size increases, which gives rise to an increased penetration of fluid into the porous block. As is show in figures 12 & 4, enhancement of heat transfer in a porous blocks in comparison to a smooth channel is not pronounced. For these heater blocks, there exist interblock recirculation lows, which weaken the penetration of fluid into porous blocks. In case of most downstream heaters 5, the penetration of fluid into the block is minimal and heat transfer is mostly conducive within the block. The results of plots of PPI vs Darcy number in figures 10-12 show a decrease in Darcy number with increasing poresize, The Darcy number has a profound effect on modulation type. The Nusselt number increased with distance from heater due to higher heat transfer near wall due to higher temperature of the fluid.

REFERENCES

- [1] J.H.Bae; Numerical Heat Transfer, **14**, 897-905 (2003).
- [2] N.H.Saeid, I.Pop; Int.Comm.Heat and Mass Transfer, **9**, 718-730 (2002).
- [3] Baytas, Pop; Journal of Thermal Sciences, **8**, 332 (2000).
- [4] E.M.Sparrow; J.of Heat Trans., **81(2)**, 157-165 (1959).
- [5] A.Bahoul et al.; Int.Comm.Heat and Mass Transfer., **32(6)**, 795-797.
- [6] S.R.DeGroot, P.Mazur; 'Non Equilibrium Thermodynamics', North Holland, (1969).
- [7] J.Estebe, C.R.Schott; Acad.Sc.Paris, 271.
- [8] N.Mendes, Phillpi, Lamberts; Int.J.of Heat and Mass Tr., **45**, 509-518 (2002).
- [9] ASHRAE; Handbook Fundamentals - American Society of Heating Refrigeration and Air Conditioning Engineers, Atlanta, (1993).
- [10] K.Clausius, G.Dickel; Naturewise, **5**, 345 (1938).
- [11] Aldok; 'Relaxation Method in the Solution of Partial Differential Equations', McGraw-Hill, N.Y., (1942).
- [12] L.V.Kantrovitch, V.I.Krylov; Approximate Methods of Higher Analysis, Wiley Newyork, (1960).
- [13] J.V.Beck, K.D.Cole; Heat Conduction using Greens Functions, Hemisphere Publishing Corp, Washington, DC, (1992).
- [14] Peaceman, Rachpover; J.of Soc.for Ind.and Appl. Maths, **3**, 28-41.
- [15] A.Haji-Sheikh et al; Int.J.of Heat Mass Tr., **47(9)**, 1889-1905 (2004).
- [16] A.Haji Sheikh, W.J.Minkowycz, E.M.Sparrow; Int. J.of Heat Mass Tr., **47(22)**, 4685-4689 (2004).
- [17] J.H.Bae; J.of Heat Transfer & Thermal Engg., **5**, 892-905 (2003).
- [18] D.Q.Kern; Process Heat Transfer, 2nd Edn, 331 (1979).